ELSEVIER

Journal of Chromatography A, 888 (2000) 1–12

JOURNAL OF CHROMATOGRAPHY A

www.elsevier.com/locate/chroma

Physical evidence of two wall effects in liquid chromatography

R. Andrew Shalliker[a,b,c], B. Scott Broyles[a,b], Georges Guiochon[a,b,*]

[a]*Department of Chemistry, The University of Tennessee, Knoxville, TN 37996-1600, USA*
[b]*Chemical and Analytical Sciences Division, Oak Ridge National Laboratory, Oak Ridge TN 37831-6120, USA*
[c]*Faculty of Science and Technology, CBBR, University of Western Sydney, Hawkesbury, Richmond, NSW 2753, Australia*

Received 18 February 2000; received in revised form 25 April 2000; accepted 26 April 2000

Abstract

Using optical on-column visualization for the study of the migration of sample bands, the radial variations of the local migration rate were studied in the region near the column wall. Photographs of small sample bands migrating along the column at various radial locations were obtained. On-column chromatograms extracted from these photographs showed evidence of two wall effects. The first of these effects was present only within the immediate vicinity of the wall. It is a direct result of the inability of the packing material to form a close packed configuration against the rigid column wall surface. The second wall effect causes a systematic variation of the migration rate of the sample band in the region of the wall, this rate increasing from the wall to the central region of the column. The corresponding images portrayed the classical ''wall effect'' that chromatographers have long discussed. They also show that this effect extends further into the column than anticipated. As to what are the relative contributions to the results of our observations of the wall effect and of a frit effect discussed in previous publications, this could not be ascertained. © 2000 Elsevier Science B.V. All rights reserved.

Keywords: Wall effects; Visualisation of wall effects

1. Introduction

Chromatographers have argued for years about the ''wall effect''. It was never clear, however, what they actually meant by that. There was, until now, no concrete and especially no visual evidence to illustrate such an effect, even though there was sufficient circumstantial evidence to postulate it as real. However, this evidence points toward two different effects and none yet has really been demonstrated in chromatography. The wall can interact with the packed bed in two different ways which are simple to understand but whose consequences are harder to figure out.

The first and most obvious interaction is purely geometrical. The bed is packed with quasi-spherical particles having a narrow size distribution and an average size which is several orders of magnitude smaller than the column diameter. The wall is flat and smooth, with a rugosity which is at least one order of magnitude smaller than the particle diameter. So, particles can touch the wall, they cannot penetrate it. In the immediate vicinity of the column wall, at a distance of the wall smaller than one particle radius, the void fraction of the bed becomes larger than its average inside the bed. It tends toward 1 at the wall. It is a minimum at a distance of the wall equal to one particle radius and, over a distance

*Corresponding author. Fax: +1-865-974-2667.
E-mail address: guiochon@utk.edu (G. Guiochon).

0021-9673/00/$ – see front matter © 2000 Elsevier Science B.V. All rights reserved.
PII: S0021-9673(00)00517-3

of a few particle diameters, it oscillates toward the average value found in the core of the packed bed. The amplitude of these oscillations decays rapidly. This phenomenon was abundantly documented in chemical engineering [1–4]. A good functional description of the variations of the bed fraction with the distance to the wall is available [3]. The mobile phase velocity increases very rapidly with increasing void fraction [5]. The Blake–Kozeny equation [5] shows that it will be nearly two orders of magnitude larger along the wall than its average value inside the bed. To the extent of our knowledge, this effect was mentioned once in the chromatographic literature, by Golay in 1959 [6]. As it affects a very thin region of the bed and does not seem to be a plausible culprit for serious losses of separation power, it has remained forgotten, although it could very well be responsible for the low efficiency reported by Knox for columns having a diameter equal to a dozen or so particle radii [7–9].

The second interaction between the bed and the wall is caused by friction between the bed and the column wall [10,11]. It is long known that chromatography columns are radially heterogeneous. Systematic studies by Knox [12], Eon [13], Baur et al. [14,15] and Farkas et al. [16–18] demonstrated that. Knox suggested that the region of the bed affected by this second ''wall effect'' is about 50 particle diameter thick [12] and Eon agreed [13]. For small preparative columns, the region affected was found to be thicker [18]. No data are available for wide bore columns, however. More recent studies using NMR measurements of the local dispersion coefficients [19,20] showed that the local bed efficiency is high across most of the column bed. However, the warping of the radial profile of the band caused by the radial velocity distribution results in a poor efficiency if measured on the elution peak, in the bulk eluate. This warping arises mostly around the column wall but it may take place also in other locations which appear to be fault lines in the packed bed [19]. The fractional volume of the column affected by this second wall effect is larger than that affected by the first one, by nearly two orders of magnitude for any column but microbore ones. It is large enough to affect markedly the separation power of columns.

Two comments must be made at this stage. First, the sample distribution may not be always homogeneous across the column head. The injection band may not enter everywhere across the column inlet at the same time either [21]. Lack of radial homogeneity of the injection band and of radial synchronicity of the injection could explain some of the results reported above but not all of them. The confirmation of the results obtained by local detection across the column exit [12–18] by (1) other data showing a flat radial profile of the injected density (amount injected per unit surface area) [15–18]; (2) NMR data [19,20]; and (3) optical visualization [22–24] demonstrates that an incorrect injection or a faulty distributor are not the only important causes of the radial distribution of the mobile phase velocity. Yet, frit effects also may play a significant role [25]. Secondly, all what these studies indicate is that the length-average flow velocity in the central region of the column is 2 to 8% higher than near the wall and that the local efficiency is up to several times higher in the center than along the wall [12–18]. We have no estimate of the possible axial variation of this velocity distribution. However, because of the limited amplitude of the radial variations of the average velocity, a precision of 1% would be required for the local velocity measurements in order to investigate fruitfully the axial distribution of the velocity at various radial locations. Data obtained by optical visualization cannot deliver this level of precision at present [23,24].

In summary, we know that columns are not homogeneous. We suspect that, in a thin layer of the bed, just against the wall, the mobile phase velocity is high and that, in a thicker layer inside this first one, the mobile phase velocity is slightly lower than its average in the whole column. We have no real proofs that these layers do exist, however. Although the properties of the first layer are probably approximately constant along the column length because of the geometrical origin of this layer, we do not know how the properties of the second layer vary along the column. We know little about the mechanism of formation of this latter layer, except that it is related to friction [11] and we have no idea how to reduce its extent nor its deleterious influence on column efficiency. We do not know either the extent of the influence of the former layer on column performance. For example, it might contribute to peak

tailing. This ignorance explains an intriguing paradox of column technology. On the one hand, considerable progress were made during the last twenty years in developing high quality packing materials [26–29]. Modern materials have nearly spherical, smooth particles with narrow particle size distributions, easily accessible pores, and the chemistry of their surfaces is highly reproducible, so data acquired with them are highly reproducible [27–29]. On the other hand, the efficiency of present day columns is only marginally better than that of columns packed a score ago [26–29]. We are of the opinion that the underestimation of the significance of the wall effects has considerably contributed to this lack of progress of column packing technology.

To improve the packing process, we must understand the existence of the wall effect, its origin, and its interaction with the chromatographic process. This study is a step in that direction. Whether the packing process is by slurry packing (analytical and some preparative columns) or dynamic compression (preparative columns), it involves the application of a high level of stress to force the particles into a consolidated bed and minimize the dead volume between the particles. Hydrostatic pressure on the bed or viscous drag of the particles in slurry packing have the same effect as mechanical stress in dynamic compression [11]. During the consolidation stage which follows, friction between the particles [30] disperse the local stress and eventually directs it toward the column wall. Because of these frictional forces, of the resulting radial stress that forces the particles against the wall and of the friction between the bed and the wall [11], a higher packing density is established in the wall region. Consequently, the bed permeability is higher in the central region than near the wall and a heterogeneous radial flow velocity distribution takes place. This explains the second ''wall effect''. During hydraulic consolidation, the external porosity of the bed decreases linearly with increasing pressure between 72 and 770 atm (1 atm=101325 Pa) [31]. Yet, the radial stress and the wall friction prevent the bed from consolidating further, once the bed has formed and particles lost any mobility. A direct illustration of this apparent contraction was shown in columns placed in an ultrasonic bath after having been packed under high pressure. Further bed consolidation in the ultrasonic field could take place only under low inlet (hydraulic) pressure [32].

The goal of this study was essentially to visualize the behavior of small, point-like bands migrating along a column. We employed a visualization method previously developed [22–24], using glass columns containing a mobile phase and a stationary phase with the same refractive indices, so that we could visualize the behavior of bands of iodine (unretained) in the vicinity of the column wall. In a separation system where both phases have the same refractive indices, the otherwise opaque bed becomes transparent to the eye and the camera, allowing the study of the three-dimensional migration of bands of colored solutes. Studying the migration behavior of such small bands would provide information regarding the radial distribution of the local velocity of the mobile phase. We present here results illustrating the complex nature of the wall effect.

2. Experimental

2.1. Chemicals

All solvents were used as supplied from the manufacturers. Reagent-grade carbon tetrachloride was purchased from Sigma (St. Louis, MO, USA). HPLC-grade dichloromethane and HPLC-grade methanol were obtained from Fisher Scientific (Fairlawn, NJ, USA). Iodine (99.9%) was obtained from General Chemical Division (New York, NY, USA). The stationary phase was YMC 15–30 μm C_{18} chemically bonded silica (YMC, Wilmington, NC, USA). Attentive care was taken when handling carbon tetrachloride, due to its toxic and carcinogenic effects. All work was performed in a well ventilated hood and protective precautions taken as prescribed by the Material Safety Data Sheet (MSDS).

2.2. Columns

All chromatographic experiments were performed on a 100×17 mm (I.D.) borosilicate (Pyrex) glass column (refraction index, $n=1.473$) supplied by Omni (Cambridge, UK). The column end fittings were prepared by the University of Tennessee work-

shop and machined from Delrin plastic. These fittings included a fixed length outlet fitting and an adjustable inlet fitting that allowed axial compression of the column. High-molecular-mass polyethylene frits were inserted into the end fittings. The stationary phase used was YMC C_{18} silica (Kyoto-Fu 613, Japan). This material is spherical with a particle size distribution given as 15–30 μm and an average particle size of 21 μm. The column was slurry packed in a downward configuration using conditions previously described [22–25]. The column was compressed under a torque of 0.2 m·kg and allowed to rest overnight. The head fitting was then carefully removed and the inlet fitting that allowed for wall injections was then inserted (see below). To improve visualization and minimize the cylindrical lens effect, the entire column assembly was placed into a laboratory-prepared, rectangular, box-shaped, viewing cell filled with what was initially intended to be carbon tetrachloride (n=1.460). For occupational safety reasons, and because the optical distortion due to the cylindrical lens effect is a function of the difference of the indices of the solvent in the column and the solvent in the viewing box, much less toxic dichloromethane (n=1.424) was used instead. The cell assembly was described previously [22] and the ramifications of using dichloromethane in the cell assembly have been discussed in detail previously [23].

2.3. Sample injection

Unless otherwise specified, iodine dissolved in carbon tetrachloride (12 g/l) was used as the probe solute. In this mobile phase, iodine is practically unretained. At this concentration, the solute zone is sufficiently colored and allows the detailed observation of the zones obtained upon the injection of the small volumes (less than 20 μl used in this work) during their entire elution. Sample injection in the vicinity of the wall was achieved using a modification of the central point method previously described [22]. A needle was inserted in the inlet frit and then bent at an angle so that sample could be loaded at the desired radial location. This head fitting was then inserted into the bed, with minimal disturbance to the column inlet. Fig. 1 illustrates the head fitting design and the location of the sample introduction needle with respect to the column wall and inlet frit.

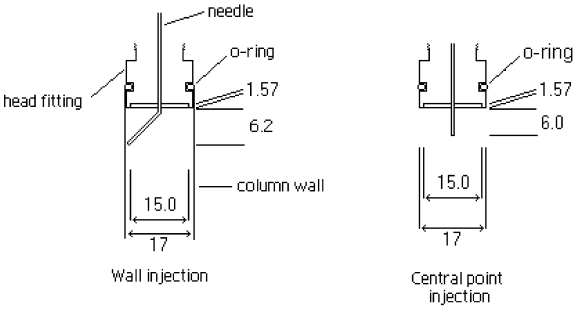

Fig. 1. Diagram of the inlet head fitting showing the relationship between the column wall and the sample introduction. All dimensions are in mm. Further details can be seen in the photographs in Fig. 2. See also refs. [20–23].

2.4. Equipment

The chromatographic system consisted of two high-performance liquid chromatographic (HPLC) pumps (model 510, Waters Associates, Milford, MA, USA) controlled by a Waters automated gradient controller. The mobile phase was 100% carbon tetrachloride and the flow-rates are specified in the appropriate figure captions. Sample visualization of the band profiles was achieved using two Pentax ZX-M SLR 35 mm cameras fitted, one with a Promaster 100 mm macro lens, the other with a Makinon 80–200 mm macro zoom lens. Kodak Ektachrome 200 ASA Professional slide film was used throughout. The photographic images were digitized using a Nikon CoolScan II (Nikon, Melville, NY, USA) film scanner. All images were acquired at the maximum resolution of the scanner (2700 dots per inch). Adobe Photoshop 5.0 (Adobe Systems, San Jose, CA, USA) was used to perform image manipulations (i.e., picture enlargement background subtraction). Further analysis was done using SigmaScan Pro 4.01 (Jandel Scientific, San Rafael, CA, USA) image analysis software.

2.5. Data analysis.

The process of data analysis was discussed in previous communications and is beyond the scope of

this communication. For further information, see Refs. [22–24].

3. Results and discussion

The photographs in Fig. 2a–d show the migration of a sample band along the central region of the column. Migration occurs according to the infinite diameter column model [8,33]. Note that, during the sample migration, the band remains uniform in shape, practically spherical throughout its entire migration. This is confirmed by the complementary set of photographs taken by the camera at right angle of the one with which the photographs in Fig. 2 were taken (not shown). The band profiles shown in Fig. 3 were extracted from the photographic information, using our normal procedures, except that the data shown are profiles of grayscale intensity and were not converted into concentration distributions. This is of little consequence in this case because we have not attempted to extract information regarding the sample distribution or the column efficiency. Previous studies have indicated that, because of the nonlinear relationship between concentration and grayscale intensity, the actual band profile is narrower than the profiles shown in the figures [23]. Nevertheless, these profiles clearly show the symmetry of the migrating sample band and the constancy of the migration rate of the sample across this region

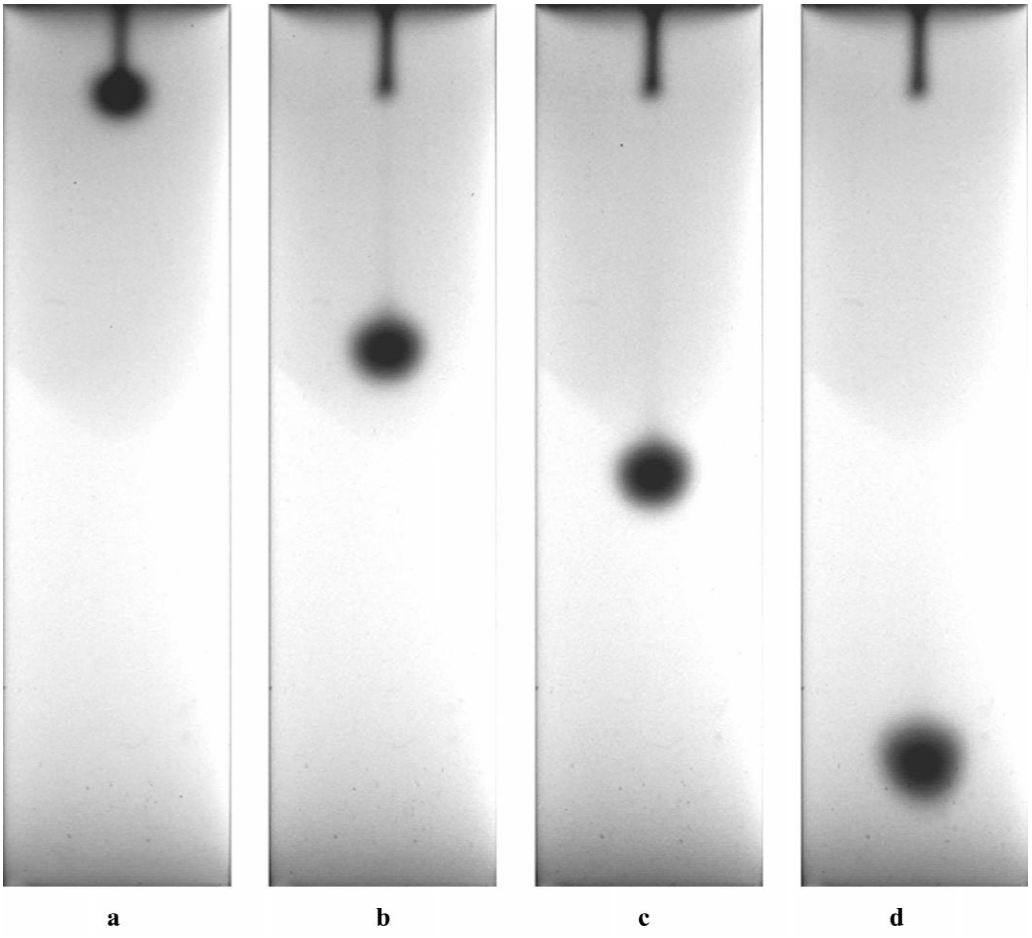

Fig. 2. Photograph of a 20 μl solution of iodine migrating along a chromatography column following a central point injection. Flow rate: 1.5 ml/min. (a) Initial injection, time = 0; (b) time = 1.75 min; (c) time = 2.60 min; (d) time = 4.60 min.

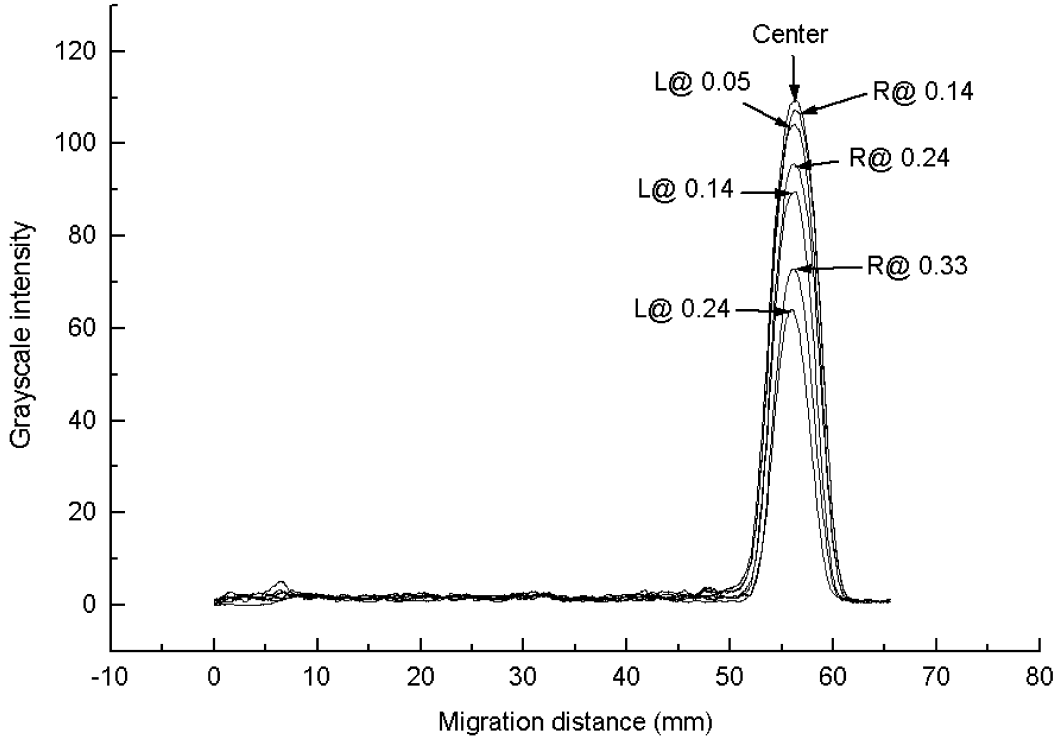

Fig. 3. Migration band profiles extracted from the photograph in Fig. 2d. The seven profiles represent the axial distributions of the grayscale intensity along the center of the band and along three sections on both the left hand side (L) and the right hand side (R) of the band, at the radial locations indicated as fractions of the column radius, *R*, and measured from the column center. These profiles were not corrected for the variable path length and reflect only the consistency in migration rate and sample dispersion.

of the column. Since iodine is unretained, band broadening is essentially by dispersion and, at this flow-rate, radial dispersion proceeds only slightly faster than axial dispersion.

In stark contrast, the photographs in Fig. 4a–f show the migration of a sample band in the wall region of the column. The sample was injected in a manner such that its band would touch the column wall. In Fig. 4a, the sample was just introduced and its profile is nearly hemispherical, almost flat on the side where it touches the wall. Actually, it is cylindrical but the cylinder radius, being that of the column, is more than ten times as large as that of the sample. Carried downstream by the stream of mobile phase, the sample migrates and the series of photographs in Fig. 4b–e illustrate the two wall effects. These will be discussed separately. Fig. 4f was obtained at right angle to the other five figures. It shows a slightly distorted elliptical profile, symmetrical by respect to the figure axis. Although the fast moving diffuse front at the wall is visible also from this angle, the second wall effect and the radial heterogeneity of the mobile phase flow are hidden. This figure demonstrates the usefulness of dual camera detection.

Regarding the first wall effect, the photographs in Fig. 4 show that the part of the sample which is in the immediate vicinity of the wall migrates at a rate that is much greater than that of the bulk sample migration. This explains the unusual shape of the band in Fig. 4c–e, with a long, narrow line against the wall and a broader, shorter line slanted toward the inside of the bed. In Fig. 4d, the radial profile of the zone has the shape of an upside down tick mark while in Fig. 4f its profile has a heart shape. This illustrates that a small yet significant amount of the sample moves fast along the wall. This phenomenon can also be clearly observed in the migration profiles

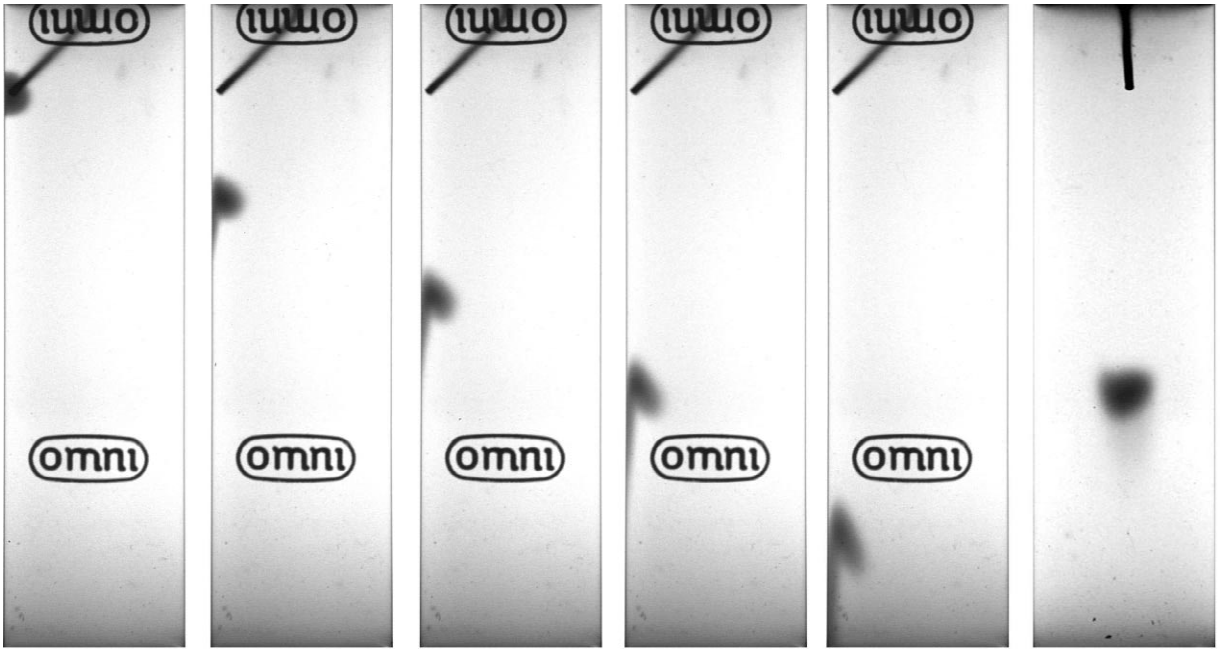

Fig. 4. Photograph of a 10 μl solution of iodine migrating along a chromatography column, following an injection close to the wall. Flow rate: 1.5 ml/min. (a) Initial injection, time = 0; (b) time = 1.00 min; (c) time = 2.00 min; (d) time = 3.00 min; (e) time = 4.60 min; (f) time = 3.00 min. Photo taken at a right angle to (d). Note the two wall effects. The first one leads to a very high rate of migration of the band in the region in the immediate vicinity of the column wall, the second to an increasing rate of migration of the band with increasing distance from the wall.

shown in Fig. 5. These profiles exhibit detectable peak fronting at radial locations greater than approximately $0.8R$.[1] The degree of peak fronting increases with decreasing distance from the wall. From Fig. 4b–e, it is not possible to determine exactly how far from the wall this effect extends. However, the degree of peak fronting begins to be significant for the migration profiles obtained at radial locations of about $0.9R$ (Fig. 5), that is, 0.85 to 1 mm from the column wall. This amounts to a depth of 40 to 50 particle diameters, assuming an average particle size of 21 μm. This figure would be too large for a wall effect of the first type if it were not to be considered in view of a very fast transverse dispersion caused by the extremely steep concentration gradient arising from a first wall effect. Assume that a layer of iodine solution of uniform and negligible thickness (ca. one particle radius, 10 μm) is placed along the column wall under static conditions. The molecular diffusion coefficient of iodine in carbon tetrachloride is approximately[2] $2.75 \cdot 10^{-5}$ cm^2/s. In a packed bed, the apparent diffusion coefficient would be 0.75 times as much. In the time it takes for the band to move from the column inlet to its position when Fig. 4d is recorded (3 min), the layer has become approximately 0.85 mm thick. This is in excellent qualitative agreement with the experimental results in Fig. 4. Therefore, this figure demonstrates the first wall effect. Note also that the experiments being

[1] All radial locations are measured from the column axis toward the wall.

[2] Using $\eta = 0.86$ cP, $M_B = 154$ g/mol, and $V_A = 63.5$ cm^3/mol (which assumes a density of 4 g/ml for liquid iodine at its melting point of 116°C), the Wilke and Chang equation [34] gives $D = 2.65 \cdot 10^{-5}$ cm^2/s at 300 K. With the same data, the Scheibel equation [35] gives $D = 2.75 \cdot 10^{-5}$ cm^2/s. A bed tortuosity of 0.75 is assumed.

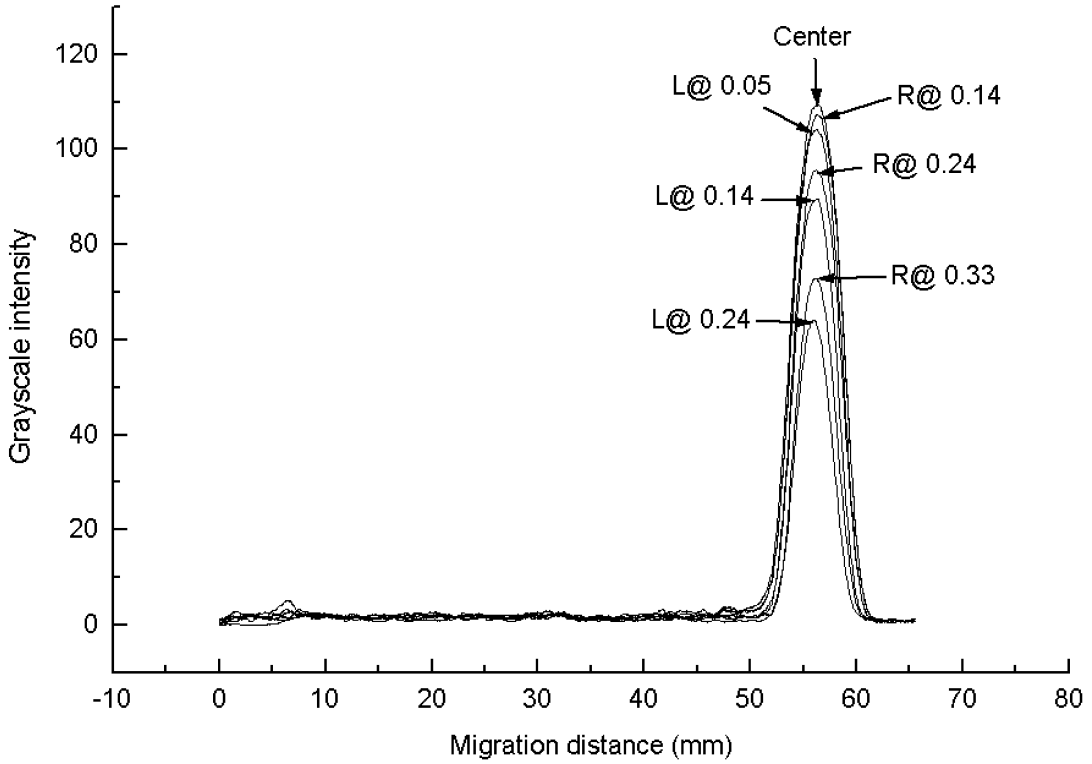

Fig. 5. Migration band profiles extracted from the photograph in Fig. 4e. The nine profiles represent the axial distributions of the grayscale intensity along sections of the band profile parallel to the column axis, at radial distances approaching 1.0, i.e., close to the wall. These profiles were not corrected for the variable path length (see Fig. 3).

carried out at a flow-rate of 1.5 ml/min, we have $u=0.016$ cm/s (with $\epsilon=0.80$), hence $v=1.2$, a rather low reduced velocity which explains the nearly spherical shape of the zones obtained with a centrally injected sample (Fig. 2).

The second wall effect is also observed in the photographs shown in Fig. 4. Initially, the sample is loaded onto the column as a quasi-hemispherical band (Fig. 4a). It rapidly distorts into a tick mark shape as migration proceeds (Fig. 4b–e). The central fraction of the sample migrates more slowly than the fractions which are either closer to the center of the column or nearer to its wall. This is consistent with a lower permeability of a wall region of the column approximately 40 to 60 particle diameters thick, as typically associated with the wall effect [10,12–18]. Unfortunately, optical distortion of the photograph in the region of radial distances between R and ~$0.8R$ from the column axis makes it difficult to quantitate the migration profiles of individual profiles [22,23]. Even though image distortion prevents accurate quantitation, this distortion cannot affect the position of the maximum concentration of the band. Grayscale intensity profiles representing the concentration distributions along parallel straight lines located at various distances from the column axis between $0.50R$ and $0.95R$ in Fig. 4e were extracted from the images and are shown in Fig. 5. They clearly show that, while the migration distance within 4.6 min decreases (hence, so does the local mobile phase velocity) with increasing distance from the column axis, the fraction of the band located very close to the wall migrates at a velocity which increases rapidly with decreasing distance to the wall. This behavior was expected if a second wall effect was also present.

Fig. 6 shows a plot of the average velocity of axial concentration profiles scanned from photographs of

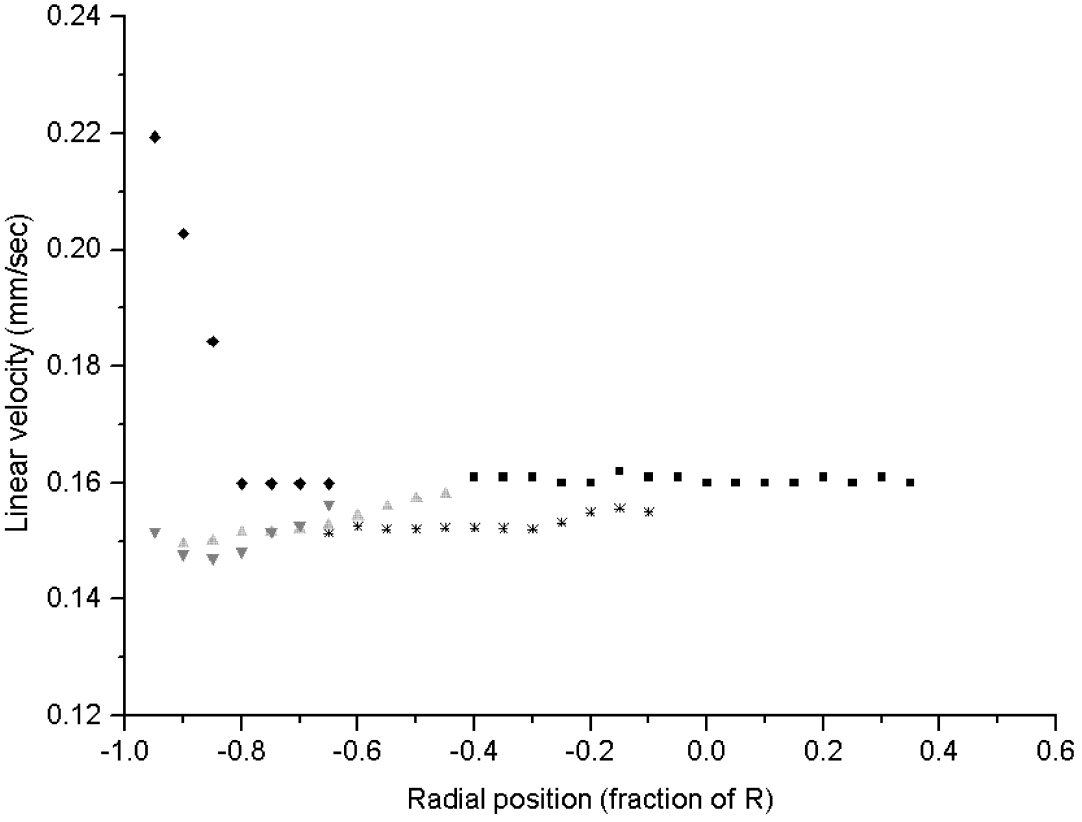

Fig. 6. Velocity distributions for local injections of small sample droplets made at various radial positions (expressed as a fraction of the radius, *R*). The migration distances used for velocity determinations were calculated from the position of the maximum peak heights, except in the last case. ■ Droplet path along the column axis. *Droplet injected at a radial distance of 0.3*R*. ▲ Droplet injected at a radial distance of 0.6*R*. ▼ Droplet injected at a radial distance of 0.9*R*, migration distance determined from the position of the peak maximum concentration. ♦ Droplet injected at a radial distance of 0.9*R*, migration distance determined from the position of the peak front at the baseline of the profile.

narrow bands, similar to those shown in Figs. 2 and 4 (but not shown), versus the radial position of the scans. These bands were injected in the column center and at various locations between the column axis and its wall. For bands injected close to the wall, different definitions of the average velocity were used. The results in Figs. 5 and 6 are in agreement. These figures demonstrate clearly a second wall effect, the average velocity between the column inlet and its wall being constant in the core region, then, beyond a radial location of 0.7*R*, decreasing slowly toward the wall, and, finally, jumping abruptly, when very close to the wall, and more than doubling (Fig. 6). This figure is not in contradiction with the assumption of a velocity orders of magnitude larger along the wall than in the core region. Transverse dispersion would be extremely fast on the scale of the effect, as shown earlier. The nature of the experiment prevents from carrying out more precise measurements of the local velocity.

At this stage, a precautionary note is in order. We cannot explicitly assume without further validation work that the radial variation of the migration rate illustrated in Figs. 5 and 6 is entirely due to a second ''wall effect'', i.e., to a systematic radial variation of the void fraction and the packing density. In several previous studies, we found an important frit effect affecting the flow profile of the mobile phase along the column. A radial variation of the mobile phase

velocity may also be a consequence of the lack of radial homogeneity of column frits (at column inlet and outlet). Admittedly, the sample is injected locally in the column, downstream from the frit. Nevertheless, the inlet frit may slightly affect the local velocity. Depending on the particular frit, the contribution can be negligible or significant compared to the phenomenon reported here. As the inlet frit used here was modified to permit the passage of the injection device (Fig. 1), it was not possible to ascertain quantitatively the contribution of the frit in this case. It is not possible to separate the two effects in the experiments of on-column visualization.

Finally, the compounded effects of the radial heterogeneity of the frit and the packed bed (including both wall effects) on the sample migration are illustrated by a comparison of the chromatograms recorded by a post-column detector as responses to the two local injections, the one made in the column center (Fig. 2) and the one made close to the wall (Fig. 4). These two chromatograms are shown in Fig. 7. Curve b in this figure shows the profile obtained for the sample injected in the column center and migrating in accordance with the infinite diameter column (Fig. 2). This profile is symmetrical, as illustrated by the overlay of a Gaussian function with the same variance, curve c, with an efficiency corresponding to $h=2.2$, calculated using the half-height method. In comparison, the sample that migrated close to the column wall gave an unsymmetrical, strongly fronting peak, showing that part of the sample traveled quickly along the immediate vicinity of the wall. The efficiency of the peak eluted from the column is much lower (curve a), with

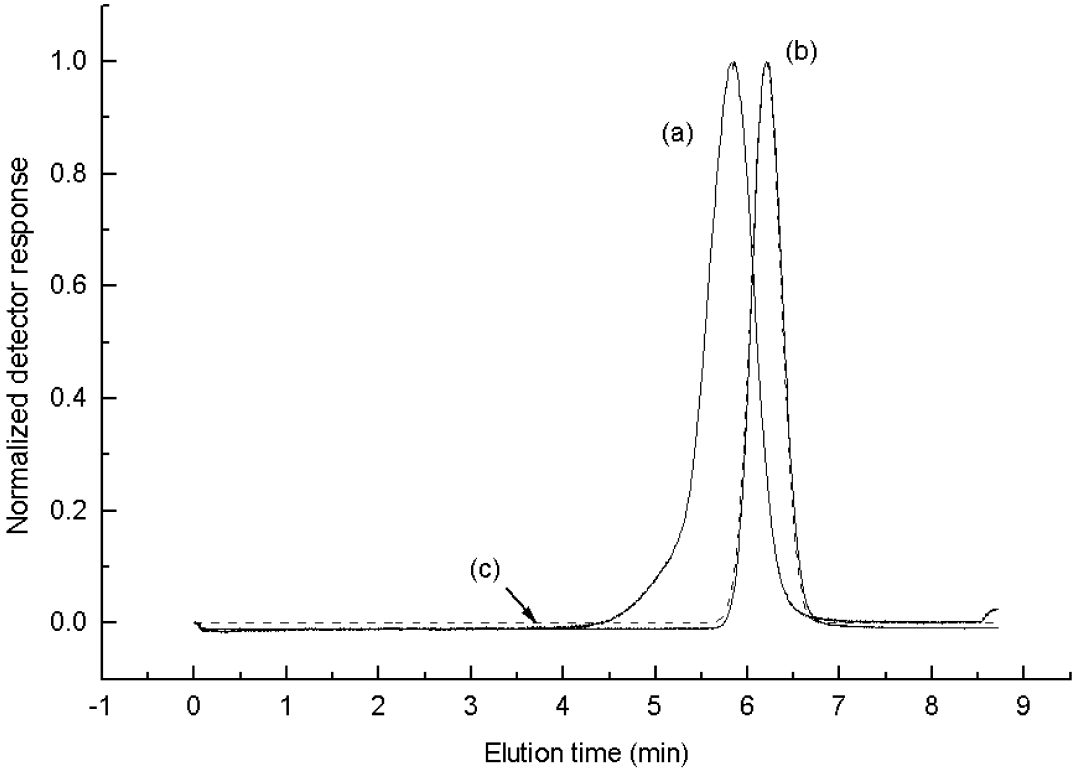

Fig. 7. Post-column chromatograms, recorded on-line with a UV detector, and normalized to their respective peak maximum, obtained for samples of ca. 10 μl (a) and 20 μl (b) of the iodine solution eluting as the result of injections made: a=close to the column wall (Fig. 4), b=in the column center. Curve c is a Gaussian function having the same variance, σ^2, as curve b. The flow-rate in each case was 1.5 ml/min. UV detection at 440 nm.

$h = 8.9$. This result is obviously consistent with the variable rate of solute migration shown in Fig. 5.

4. Conclusion

The results in this paper demonstrate for the first time that two wall effects take place in chromatographic columns. The first effect is geometrical. The mobile phase can flow around the bed of packing material, in the immediate vicinity of the wall because the particles cannot form a close packed configuration against the rigid flat surface of the wall. Although known from chemical engineers for more than 50 years, this effect was suspected by few chromatographers and was never taken into account in analyses of the separation power of columns. Dynamic radial compressed columns should not exhibit this effect if the packing particles are hard enough and the plastic sheath serving as internal tubing is soft enough for the particles to incrust themselves deeply enough into the column wall. Note that this wall effect was not observed in a recent study of the radial distribution of the mobile phase velocity in a dynamic radial compression column [36], although its absence could have been due, in part, to the relatively low definition of the NMR measurements (250 μm per pixel) compared to the average particle size (80 μm). Whether this is a worthwhile approach remains to be demonstrated, however, because we do not really know the extent of damage done to the separation power of columns by the first wall effect. If harmful, the consequences of this effect are also alleviated by the property of inlet distributors and frits to distribute the injected sample heterogeneously across the column inlet [22–24]. Mostly less sample being distributed to the wall, the wall effect becomes less important.

The second wall effect was also observed, corresponding to the classical ''wall effect'' observed by many previous workers [12–18]. The mobile phase velocity is lower in a region close to the wall, the stream being slowed by the low void fraction associated with a higher packing density near the wall caused by the high radial stress applied by the bed to the wall as a consequence of friction between particles. However, part of the effect observed might be due to a radial heterogeneity of the frits. It was not possible to separate these two effects quantitatively. Further work is in progress to elucidate further the origins and consequences of these effects.

Acknowledgements

This work was supported in part by grant DE-FG05-88-ER13869 of the US Department of Energy and by the cooperative agreement between the University of Tennessee and the Oak Ridge National Laboratory.

References

[1] S. Ergun, A.A. Orning, Ind. Eng. Chem. 41 (1949) 1179.
[2] M. Venneti, H. Govindarao, G.F. Froment, Chem. Eng. Sci. 41 (1986) 533.
[3] G.E. Mueller, Chem. Eng. Sci. 46 (1990) 706.
[4] K. Schnitzlein, Chem. Eng. Sci. 48 (1992) 811.
[5] R.B. Bird, W.E. Stewart, E.N. Lightfoot, Transport Phenomena, Wiley, New York, 1960.
[6] M.J.E. Golay, in: H.J. Noebels, R.F. Wall, N. Brenner (Eds.), Gas Chromatography, Academic Press, New York, 1961, p. 11.
[7] J.H. Knox, Anal. Chem. 35 (1963) 449.
[8] J.H. Knox, J.F. Parcher, Anal. Chem. 41 (1969) 1599.
[9] J.H. Knox, J. Chromatogr. 831 (1999) 3.
[10] G. Guiochon, T. Farkas, H. Guan-Sajonz, J.-H. Koh, M. Sarker, B.J. Stanley, T. Yun, J. Chromatogr. A 762 (1997) 83.
[11] G. Guiochon, E. Drumm, D. Cherrak, J. Chromatogr. A 835 (1999) 41.
[12] J.H. Knox, G.R. Laird, P.A. Raven, J. Chromatogr. 122 (1976) 129.
[13] C.H. Eon, J. Chromatogr. 149 (1978) 29.
[14] J.E. Baur, E.W. Kristensen, R.M. Wightman, Anal. Chem. 60 (1988) 2334.
[15] J.E. Baur, R.M. Wightman, J. Chromatogr. 482 (1989) 65.
[16] T. Farkas, J.Q. Chambers, G. Guiochon, J. Chromatogr. A 679 (1994) 231.
[17] T. Farkas, M.J. Sepaniak, G.A. Guiochon, J. Chromatogr. A 740 (1996) 169.
[18] T. Farkas, M.J. Sepaniak, G. Guiochon, AIChE J. 43 (1997) 1964.
[19] U. Tallarek, E. Baumeister, K. Albert, E. Bayer, G. Guiochon, J. Chromatogr. A 696 (1995) 1.
[20] U. Tallarek, K. Albert, E. Bayer, G. Guiochon, AIChE J. 42 (1996) 3041.
[21] Q.S. Yuan, A. Rosenfeld, T.W. Root, D.J. Klingenberg, E.N. Lightfoot, J. Chromatogr. A 831 (1998) 149.
[22] R.A. Shalliker, B.S. Broyles, G. Guiochon, J. Chromatogr. A 826 (1998) 1.

[23] R.A. Shalliker, B.S. Broyles, G. Guiochon, Anal. Chem. 72 (2000) 323.
[24] B. Scott Broyles, R. Andrew Shalliker, G. Guiochon, J. Chromatogr. A 867 (2000) 71.
[25] B.S. Broyles, R.A. Shalliker, G. Guiochon, J. Chromatogr. A 855 (1999) 367.
[26] R.E. Leitch, J. Chromatogr. Sci. 9 (1971) 531.
[27] M. Kele, G. Guiochon, J. Chromatogr. A 830 (1999) 41, 55.
[28] M. Kele, G. Guiochon, J. Chromatogr. A 855 (1999) 423.
[29] M. Kele, G. Guiochon, J. Chromatogr. A 869 (2000) 181.
[30] K. Mihlbachler, T. Kollmann, A. Seidel-Morgenstern, J. Tomas, G. Guiochon, J. Chromatogr. A 818 (1998) 155.
[31] D.P. Gervais, W.S. Laughinghouse, G. Carta, J. Chromatogr. A 708 (1995) 41.
[32] R.A. Shalliker, B.S. Broyles, G. Guiochon, J. Chromatogr. A 878 (2000) 153.
[33] J.J. Kirkland, W.W. Yau, H.J. Stoklosa, C.H. Dilks Jr., J. Chromatogr. Sci. 15 (1977) 303.
[34] C.R. Wilke, P. Chang, AIChE J. 1 (1955) 264.
[35] E.G. Scheibel, Ind. Eng. Chem. 46 (1954) 2007.
[36] U. Tallarek, D. van Dusschoten, T. Scheenen, H. Van As, E. Bayer, G. Guiochon, U.D. Neue, AIChE J. 44 (1998) 1962.